Nordic Hydrology, 18, 1987, 221-236

A Perturbation Based Model of Heat-Induced Suppression of River Ice

S. Sarraf and W. Saleh

Concordia University, Civil. Eng. Dept.,
Montréal Québec, Canada

The study of the thermal response of ice covered streams to an effluent of high temperature, or of fast moving water, has been of considerable interest to those concerned with hydraulic systems, environmental effects, and navigational routes in cold regions. The discharge of tributary thermal effluents into cold region rivers may alter the thermal and hydrodynamic conditions of ice cover progression and create reaches of open water in the ice throughout the winter season. An analytical approach, based on pertubation techniques, has been developed and tested concerning the suppression of ice cover and the migration of its fronts. The upstream and the downstream ice edges are determined for two cases of steady non-uniform flow. Conditions for the suppression of the ice cover are also obtained based on the relative positions of the upstream and downstream ice edges. Comparison with field data shows a good agreement with the formulation incorporating the thermal effluent velocity.

Introduction

The common practice of disposing of heated water into streams has always raised concerns about its effect on the aquatic environment, and the overall ecological balance. In cold region rivers, the presence of such tributary effluents of a relatively high temperature usually results in suppressing the ice cover in the vicinity of the point of discharge. If sufficient heat was introduced into the receiving stream, the ice cover may melt completely over a large distance, essentially downstream of the discharge point, for the entire winter period. The proper positioning of the heated side effluents in navigable rivers might permit an effective use of these rivers for shipping throughout the winter period. In addition, the presence of open reaches downstream of hydro-electrical power plants have major effects on their operation and overall efficiency.

The magnitude and extent of changes in river temperature distribution, due to thermal side effluent input, depend mainly upon the degree of mixing between the heated effluent and the cooler receiving flow, and the rate of heat exchange between water and atmosphere which is controlled by various climatological factors. The mixing process is dominant in the region adjacent to the point of thermal discharge. Downstream from this area, the water temperature distribution is controlled by the prevailing surface heat exchange.

Previous investigations into the problem have focused on estimating the temporal, rather than the spatial changes of temperature in a river reach. Ince and Ashe (1964) used observations from the St. Lawrence river in order to compare two finite difference approaches to calculate downstream water temperature attenuation. Evaluation of the length of the ice-free reach was first attempted by Dingman, Weeks, and Yen (1967) using a differential approach for the steady-state heat balance with constant meteorological and hydrodynamic conditions. Ashton (1979, 1984) has developed a quasi-steady state numerical simulation of the effect of a thermal effluent on ice cover suppression in the presence of a constant velocity. Analytical investigation of the upstream ice edge has not been considered in previous works, nor the conditions under which the ice cover would not be suppressed.

The present paper examines the phenomena of ice cover suppression by a side effluent through an analytical model, using perturbation techniques. The steady-state quasi-linear second order energy equation constitutes its theoretical basis. The model adresses the effect of the variability of the flow velocity on the ice cover progression or regression in conjunction with the longitudinal dispersion term. The dominant variables that govern the local melting of the ice cover are evaluated in order to predict the occurrence of ice suppression through a new proposed criterion, and to estimate the location of both upstream and downstream ice cover edges for various hydrodynamic and meteorological conditions.

Theoretical Formulation

For an incompressible turbulent flow the conservation law of heat transported and dispersed in a spatially variable river flow, under the conditions of uniform temperature distribution over the depth, can be expressed by the following partial differential equation

$$\frac{\partial}{\partial t}(\rho\, C_p DT) + \frac{\partial}{\partial x}(\rho\, C_p Du\, T) + \frac{\partial}{\partial z}(\rho\, C_p Dv\, T) \equiv$$

$$\frac{\partial}{\partial x}\left[DE_x \frac{\partial}{\partial x}(\rho\, C_p T)\right] + \frac{\partial}{\partial z}\left[DE_z \frac{\partial}{\partial z}(\rho\, C_p T)\right] - \Phi \qquad (1)$$

where

D – the flow depth
T – the water temperature
u, v – the mean flow velocity components in the x (longitudinal) and in z (transverse) directions respectively
E_x, E_z – the longitudinal and transverse mixing coefficients respectively
Φ – the heat flux at the water/air or water/ice interface.

It is assumed that there is no heat flux at the river bed. If, ρ, C_p and D are assumed to be constant, and by introducing the continuity equation, the above equation can be written as

$$\frac{\partial T}{\partial t} + u\frac{\partial T}{\partial x} = E_x\frac{\partial^2 T}{\partial x^2} - \frac{\Phi(T)}{\rho C_p D} \tag{2}$$

in which the term ($v\,\partial T/\partial z$) has been omitted due to the fact that ($v\partial T/\partial z$)<<($u\partial T/\partial x$). In addition, the assumption of full mixing of the water temperature over the cross section allowed the elimination of the $E_z(\partial^2 T/\partial z^2)$ term. The above equation expresses an interrelated equilibrium among four major processes of heat transfer controlling the stream heat balance which are: the rate of change of heat in a local water section; the advection of the heat at mean flow velocity; the heat dispersion in the longitudinal direction; the rate of heat transfer at the water/ice or water/air interface. The presence of u as a function of distance x gives this equation a quasi-linear character which requires special mathematical techniques for its integration.

The Rate of Heat Transfer, Φ

In natural stream, the temperature distribution resulting from the discharge of the heat effluent is controlled by the rate of surface heat exchange. The heat exchange at the water surface is governed by several heat transfer processes which depend upon a number of climatological factors. During winter periods, the air temperature is much lower than the water temperature, therefore, the water body looses heat to the atmosphere leading to a significant cooling of the water. For the purpose of analysis of the heat transfer process at the water surface, a definition sketch is presented in Fig. 1, for both open and ice covered water.

When the water surface is open to the atmosphere the heat flux Φ is noted as Φ_{wa} (water-air interface), and can be expressed as follow

$$\Phi_{wa} = \Phi_R - (\Phi_B + \Phi_E + \Phi_H + \Phi_S) \tag{3}$$

where

Φ_R – solar or short wave radiation
Φ_B – long wave radiation
Φ_E – evaporative heat flux
Φ_H – convective and conductive heat flux
Φ_S – heat transfer rate during the melting of snow falling on the water surface.

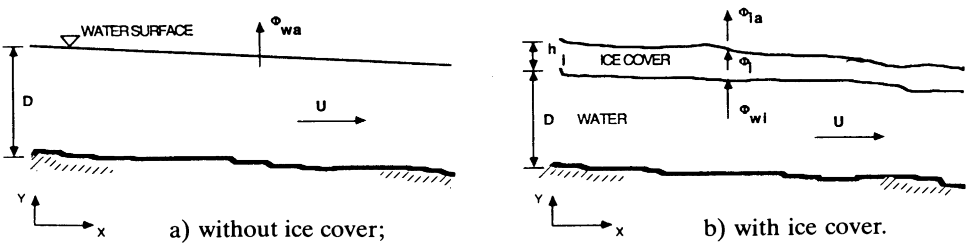

Fig. 1. Diagram of major heat transfer processes at the water surface.

Because, the surface heat flux, $\Phi_{wa}(T)$, is a complex function of the various parameters, attempts have been made to express it as a linear function in terms of water and air temperatures. In the present work, the wind velocity V_w, and air temperature T_a are considered to be the dominant climatological factors, and Φ_{wa} is therefore expressed according to the model of Edinger-Duttweiller-Geyer (1968) by the following simplified relationship

$$\Phi_{wa} = h_{wa}(T-T_a) \tag{4}$$

h_{wa} is the heat transfer coefficient applied at the water-air interface. h_{wa} has a large dependency on the wind velocity (Ashton 1979).

When the water surface is ice covered, the heat transfer consists of three major processes as shown in Fig. 1b. The heat flux to the atmosphere at the ice-air interface is given by

$$\Phi_{ia} \equiv h_{ia}(T_s-T_a) \tag{5}$$

where h_{ia} is the heat transfer coefficient at the ice-air interface; T_s and T_a are the ice surface and the air temperatures respectively. In this rather simplified model, the heat transfer coefficient h_{ia} is a function of several heat transfer parameters and wind velocity (Calkins 1984).

For the ice covered flow, the heat flux at the water-ice interface depends upon the flow hydrodynamic variables, and the heat flux Φ_{wi}, from the underside of the ice cover, can be expressed as follows

$$\Phi_{wi} \equiv h_{wi}(T-T_m) \tag{6}$$

Where h_{wi} is a heat transfer coefficient, T_m and T are the melting point (= 0°C) and the water temperatures respectively.

The classical approach to evaluate h_{wi} is based upon a closed conduit turbulent heat transfer correlation, and it can be given for open water flow in the following form

$$h_{wi} = C_{wi}\,\frac{u^{0.8}}{D^{0.2}} \tag{7}$$

where: C_{wi} varies from 1,622 to 2,433 $Ws^{0.8}m^{-2.6}\,°C^{-1}$ (Rohsen and Choi 1961).

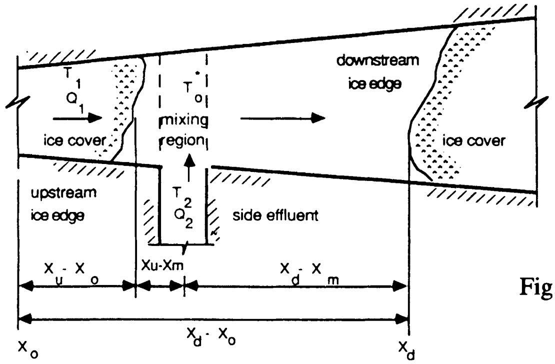

Fig. 2. Channel configuration with various geometrical locations.

Solution Procedure

Foremost among the analytical techniques are the methods of perturbations (asymptotic expansions in terms of a small or a large parameter or coordinate). According to these perturbation techniques, the solution is represented by the first few terms of a pertubation expansion, usually the first two. Although these perturbation expansions may be divergent, they can be more useful, for a qualitative as well as a quantitative representation of the solution, than expansions that are uniformly and absolutely convergent (Nyfeh 1977, 1982). In the present work, the perturbation method based on the WKB (Wentzel, Karmers, and Brillouin) approximation and the Liouville-Green transformation was used. In this manner, the effect of the flow velocity variability and the longitudinal diffusion on the ice cover suppression can be investigated. A general form of the solution is obtained for the one dimensional quasi-linear energy equation with variable flow velocity.

The configuration of the channel intersection shown in Fig. 2 is considered for the purpose of this analysis. The main channel (1) is narrow and covered with ice except in the vicinity of the intersection under favourable conditions. A uniform water temperature distribution is assumed over the cross-section, wherein, T_1 and T_2 ($>T_1$) are the temperatures in channels (1) and (2) respectively. At the intersection the ice cover might be suppressed in the main channel and an open water area may occur mainly downstream of the point of the side effluent discharge.

Open Water (downstream of the point of discharge)

For open water reach, Eq. (2) can be written as

$$u(x)\frac{\partial T}{\partial x} - E_x \frac{\partial^2 T}{\partial x^2} + \frac{h_{wa}}{\rho C_p D}(T-T_a) = 0 \tag{8}$$

In order to predict the temperature distribution along the main channel and to obtain the solution of Eq. (8), assuming

$$K \equiv \frac{h_{wa}}{\rho C_p D}$$

Denoting $\theta = K(T-T_a)$, and by differentiating with respect to x, Eq. (8) can be written with respect to θ as

$$\theta'' - \frac{u}{E}\theta' - \frac{K}{E}\theta = 0 \tag{9}$$

The solution of this second-order homogeneous differential equation, containing slowly varying coefficients, involves the use of the Liouville-Green transformation

$$\theta(x) = p(x)w(x) \tag{10}$$

Where p and w are chosen so that Eq. (9) is transformed into an equation whose dominant part has constant coefficients, i.e.

$$p''w + 2p'w' + pw'' - \frac{u}{E}p'w - \frac{u}{E}pw' - \frac{K}{E}pw \equiv 0 \tag{11}$$

By forcing the coefficients of w' to zero, gives

$$2p'w' = \frac{u}{E}pw' \equiv 0 \tag{12}$$

and Eq. (11) is reduced to

$$w'' + [\frac{p''}{p} - \frac{u}{E}\frac{p'}{p} - \frac{K}{E}]\, w \equiv 0 \tag{13}$$

Now, solving Eq. (12) for p

$$p = \exp[\int \frac{u}{2E}\, dx] \tag{14}$$

Substituting p into Eq. (13) yields

$$\frac{d^2w}{dx^2} + [\frac{u'}{2E} - \frac{u^2}{4E^2} - \frac{K}{E}]w = 0 \tag{15}$$

Further, assuming $X = x/\lambda$, in which λ is a large dimensionless parameter, Eq. (15) can be expressed in terms of the new variable X, as

$$\frac{d^2w}{dX^2} + \lambda^2 q(X)w \equiv 0 \tag{16}$$

where

$$q(X) = \frac{u'}{2E} - \frac{u^2}{4E^2} - \frac{k}{E} \tag{17}$$

Considering the nature of this second order differential equation having a large dimensionless parameter, its solution requires the use of a straightforward expansion in terms of inverse powers of λ. The WKB approximation can therefore be applied, and an expansion in the following form may be used

$$w = e^{\lambda G(X,\lambda)} \tag{18}$$

where G has a straightforward expansion in inverse power of λ, in the following form

$$G(X;\lambda) \equiv G_0(X) + \frac{1}{\lambda}G_1(X) + \frac{1}{\lambda^2}G_2(X) + \dots \tag{19}$$

Hence, evaluating w' and w'' in terms of λ and $G_i(X)$, and substituting into Eq. (16), yields

$$(G_0' + \frac{1}{\lambda} G_1' + \frac{1}{\lambda^2} G_2' + \ldots)^2 + q + \frac{1}{\lambda} (G_0'' + \frac{1}{\lambda} G_1'' + \frac{1}{\lambda^2} G_2'' + \ldots) = 0 \qquad (20)$$

Equating coefficients of λ, λ^{-1}, and λ^{-2} etc... to zero, and integrating the resulting equations, the coefficients of the expansion series are obtained. Thus, the final solution of Eq. (16) is obtained as

$$w = \exp\{\pm i\lambda \int \sqrt{q}\, dX - [\ln\sqrt{\pm i} + \ln \sqrt[4]{q}] + \ldots\} \qquad (21)$$

Next, the final expression for θ, obtained by substituting w and p in Eq. (10), is given by

$$\theta \approx \frac{c_1 \exp[\int \sqrt{-q}\, dx] + c_2 \exp[-\int \sqrt{-q}\, dx]}{\sqrt[4]{-q}} \exp[\int \frac{u}{2E} dx] + \ldots \quad q<0 \qquad (22)$$

In Eq. (22), and in subsequently following equations, only the first two terms of the expansion are retained in order to provide a practical representation of the solution. In the following section, and to provide a simple interpretation of the formulations, the solutions is given for two basic cases of non-uniform flow, namely divergent and convergent channel flows. Therefore, for a prismatic non-uniform channel, assuming velocity $u=K'^*(X-X_m)+u_m$, the solution for T, using Eq. (22), is obtained as

$$\frac{T-T_a}{T_0^*-T_a} = \frac{[\frac{\Delta}{2E} + \frac{u^2}{4E^2}]^{1/4}_{x=x_m}}{[\frac{\Delta}{2E} + \frac{u^2}{2E^2}]^{1/4}} \cdot \frac{\exp\{\frac{1}{4EK'}[u\sqrt{u^2+a^2}+a^2\log_e(\frac{u+\sqrt{u^2+a^2}}{a})-u^2]\}}{\exp\{\frac{1}{4EK'}[u\sqrt{u^2+a^2}+a^2\log_e(\frac{u+\sqrt{u^2+a^2}}{a})-u^2]\}_{x=x_m}} \qquad (23)$$

where, $\Delta = (2K+K')$, $a^2 \equiv 2E\Delta$, and $K'=(30/\rho C_p D)$.

By re-arranging Eq. (23) and after replacing T by its value at the ice edge according to the 0°C isotherm or equivalent criterion, the locations of the downstream ice cover can be obtained. These locations are shown in Fig. 3 for different water velocities.

Flow Under Ice Cover Condition

Under ice cover condition the heat flux at the ice-water interface may be expressed by $\Phi_{wi}=h_{wi}(T-T_m)$, and Eq. (2) can be written as

$$u(x)\frac{\partial T}{\partial x} - E_x\frac{\partial^2 T}{\partial x^2} + \frac{h_{wi}}{\rho C_p D}(T-T_m) \equiv 0 \quad (24)$$

Here, the heat transfer coefficient at the water-ice interface h_{wi} is a function of the water velocity and can be represented, after Rohsen and Choi (1961), by

$$h_{wi} = 1{,}622\frac{u^{0.8}}{D^{0.2}}$$

Eq. (24) is transformed into a second-order differential, but homogeneous equation which could be solved asymptotically following the Liouville-Green transformation and the WKB approximation. Therefore, by applying the same procedure as in the previous case, the final form of the solution, using the boundary conditions that, at $x \rightarrow \infty$, $q \rightarrow 0$, and at $x=X_0$, $T=T_0$, is given by

$$\frac{T-T_m}{T_0-T_m} \equiv \exp-[(\frac{u^2}{4E^2} + u^{0.80}\frac{K}{E})^{1/2} - \frac{u}{2E}](x-x_0) \quad (25)$$

with $K \equiv \frac{1{,}622}{\rho C_p D}$

Open Water (upstream of the point of discharge)

Usually a small open water area is encountered upstream of the point of effluent discharge as a result of the migration of the thermal effluent in the upper layer of the stream. Since the effluent is warmer than the ambient river temperature, and depending on the relative magnitude of the effluent velocity, a stratification and a partial upstream flow is established in the upper layer of the stream adjacent to the ice cover. In the present study, this phenomenon is regarded as a heat diffusion process in the upstream direction. The retarding effect on the main flow is accounted for through the introduction of an apparent dispersion coefficient E. Hence, for the open water reach upstream of the point of discharge, the energy balance can be formulated as follows

$$E\frac{\partial^2 T}{\partial x^2} = \frac{\Phi}{\rho C_p D} = \frac{h_{wa}}{\rho C_p D}(T-T_a) \quad (26)$$

Solving this equation for the boundary condition that, at $x = x_m$, $T = T_0^*$, and rearranging yields

$$x_u - x_m = \frac{\log_e[\frac{T_e-T_a}{T_0^*-T_a}]}{[\frac{h_{wa}}{\rho C_p DE}]^{1/2}} \quad (27)$$

Where x_u is the upstream ice edge location; x_m is the location of the point of discharge; T_e the water temperature at the ice edge, assumed to be zero according to the 0° C isotherm criterion.

Ice Cover Suppression Criterion

When the thermal exchange through the ice cover is negative, the heat, lost by the ice cover, causes its melting and suppression. The suppression of the ice cover is determined by evaluating separately the locations of the upstream and the downstream ice edge based on the equivalent isotherm criterion. Both locations occur under open water conditions.

The criterion for ice cover suppression is fixed according to the ratio R of the distance of the upstream ice cover edge from a chosen datum point x_0, to the distance of the downstream ice cover ice edge from the same datum. For the ice cover to be suppressed, $R<1$, that is

$$R = \frac{x_u - x_0}{x_d - x_0} < 1 \tag{28}$$

where, x_u- the upstream ice cover edge location; X_d- the downstream ice cover edge location; x_p- the datum point on the ice cover reach taken at a relatively large distance upstream of the thermal discharge section in a such way that $(x_u-x_0)/(x_d-x_0)$ is positive. In addition, having $R \geqslant 1$ simply indicates no suppression of the ice cover. Expanding R yields

$$\frac{x_u - x_0}{x_d - x_0} = \frac{x_m - x_0}{x_d - x_0} + \frac{x_u - x_m}{x_d - x_0} \tag{29}$$

where x_m is the location of the side discharge. Similarly, the right hand side terms of Eq. (29) may be expressed by

$$\frac{x_d - x_0}{x_m - x_0} = \frac{x_d - x_m}{x_m - x_0} + \frac{x_m - x_0}{x_m - x_0} = \frac{x_d - x_m}{x_m - x_0} + 1.0$$

$$\frac{x_d - x_0}{x_u - x_m} = \frac{x_d - x_m}{x_u - x_m} + \frac{x_m - x_0}{x_u - x_m} \tag{30}$$

All the above terms will be replaced by their analytical expressions developed earlier, in order to formulate R in terms of the hydrodynamic and thermodynamic variables, using the equivalent isotherm criterion to approximate T_e:

Discussion of the Formulations

Fig. 3 shows the location of the downstream edge of the ice cover (x_d-x_m) as a function of the initial mixing water temperature T_0^* for various air temperatures. For the purpose of interpretation, the water depth was taken as 5 m with an initial water velocity of 0.3 m/sec. The linearity of the curves is peculiar to low air and mixing water temperatures. For different air temperatures there exists a certain value T_0^* at which the curves begin to behave non-linearly. This indicates that at low air temperatures the effect of the mixing temperature is reduced and the advance of the ice cover edge is attenuated. The downstream distance to the ice

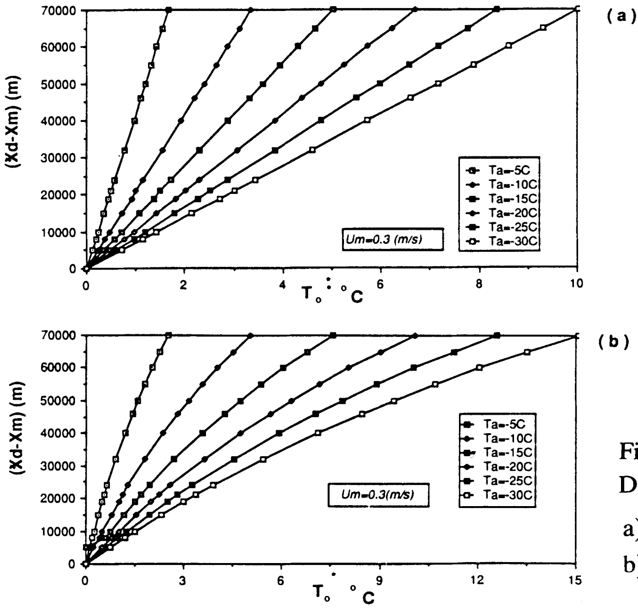

Fig. 3.
Downstream ice edge locations;

a) convergent flow;

b) divergent flow.

cover edge (x_d-x_m) increases with an increase in the air or effluent water temperature. Although the values of (x_d-x_m) shown in Fig. 3b, for divergent flow, are lower than those calculated under convergent flow conditions (Fig. 3a), the curve characteristics are rather similar.

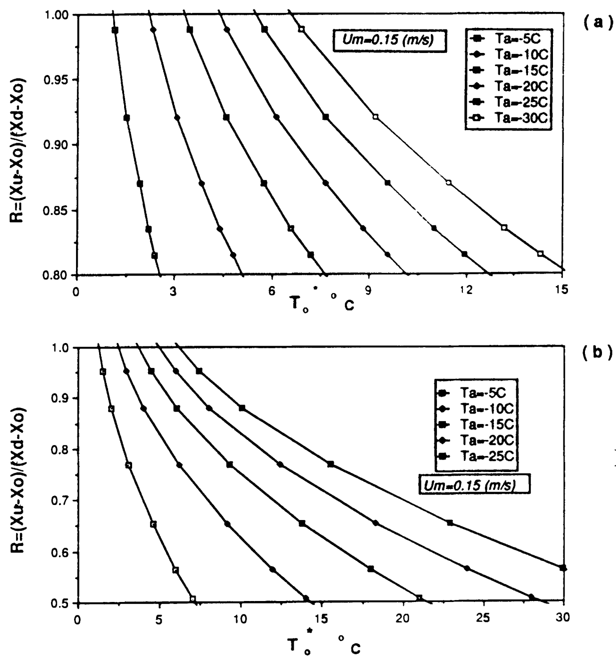

Fig. 4.
Calculated ice suppression ratio for u ≡ 0.15 m/sec.;

a) convergent flow;

b) divergent flow.

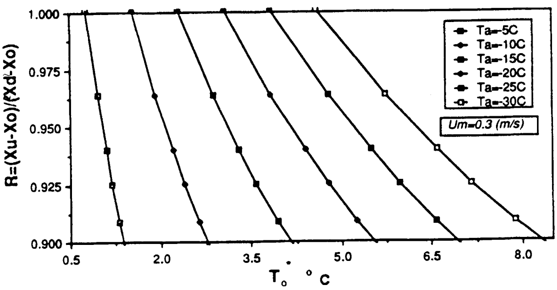

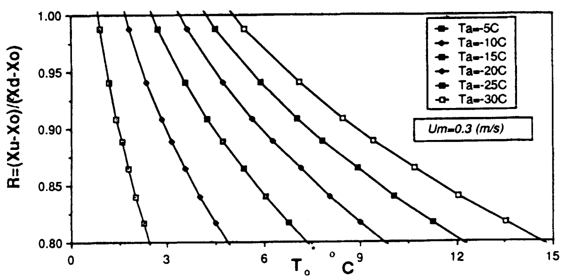

Fig. 5.
Calculated ice suppression ratio for u ≡ 0.30 m/sec.;

a) convergent flow;

b) divergent flow.

The suppression of the ice cover determined according to the ratio R is presented in Figs. 4 and 5 in terms of initial water mixing temperature for various air temperatures with initial water velocities of 0.15, and 0.30 m/sec. These figures show the effect of the variation of receiving stream velocity on the ice cover, outlining the various conditions for ice cover suppression. The linear behaviour of the curves, at low air and initial mixing temperatures, implies that at higher values of $T_0{}^*$, the effect of the freezing air temperatures T_a is diminished. Furthermore, for each air temperature, there exists a value $T_0{}^*$ at which the ice cover would be suppressed. In a convergent channel, a much lower value of the initial mixing temperature is required to suppress the ice cover under given meteorological conditions. For instance, Fig. 4a shows that, the ice cover suppression will occur at $T_0{}^* = 2.3$°C for an air temperature of −10°C and an initial flow velocity of 0.15 m/sec, where under divergent channel condition the suppression will take place at $T_0{}^* = 2.6$°C. The effect of variability in the flow velocity is shown to be more significant at lower air temperatures.

Field Measurement and Model Testing

In the winter of 1982/83, Hydro-Québec undertook a field survey project to study ice problems in the Lake St. Louis area of the St. Lawrence river (see Fig. 6). In this stretch of the river, two distinct zones are identified. The first situated upstream of Lake St. Louis with an average flow of 8,400 m^3/s, where the extent of the stable ice cover varies significantly from year to year. The second zone covers the Lachine rapids and remains mostly ice free except for a few areas of shore ice.

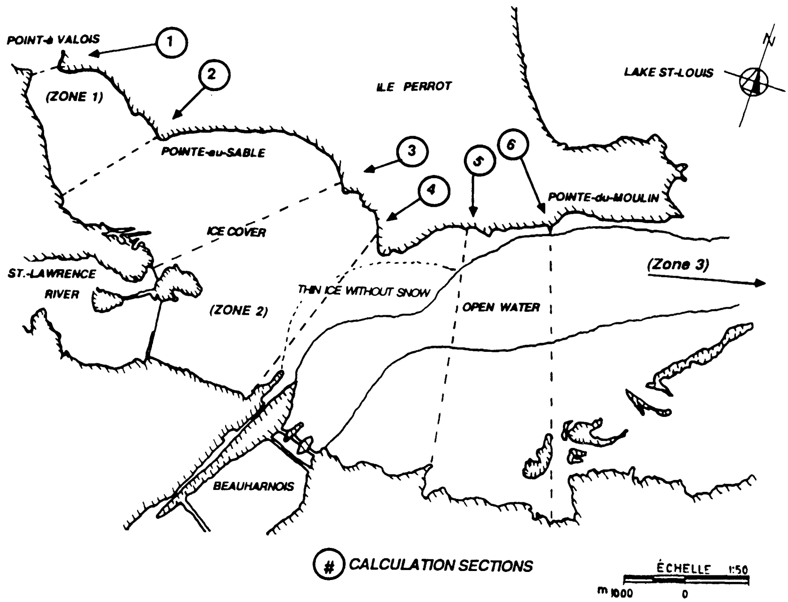

Fig. 6. Area map of the intersection of Beauharnois channel and Lake St. Louis.

The main objectives of the field study were: a) observation of ice cover formation by analyzing photographs and charts of the ice sheet in the region concerned, b) measurement of local water temperature and velocity and its variation at a number of observation sites, and c) determination of periods of formation of frazil. Visual observations and aerial photographs were used to draw complete ice maps of the area. Measurement of the water temperature was made possible by the use of a helicopter equipped with pontoons. A series of flow velocities, measured at various depths, were collected at several observation sites. Accurate temperature readings had to be taken behind wooden shields, and by using non-adhesive material for thermometer rods, in order to overcome difficulties caused by high water velocities and perturbations produced by the ice.

To check the validity of the present work, the model is tested against the collected field data for the winter period of 1982-1983. Topographic and bathymetric maps were analysed to determine the water depth along different sections. Meteorological variables collected at the nearby Dorval airport station were used. The effluent source temperature was recorded just downstream of Beauharnois power plant.

Using the above information, two types of calculation were carried out. The first was accomplished by taking the thermal effluent temperature as it is given at the source and using it in the calculations as T_0^*, assuming no mixing with the upstream water of Vaudreuil channel. The second type uses a full mixing assumption. A good agreement was achieved with the field data using both methods. Both types of

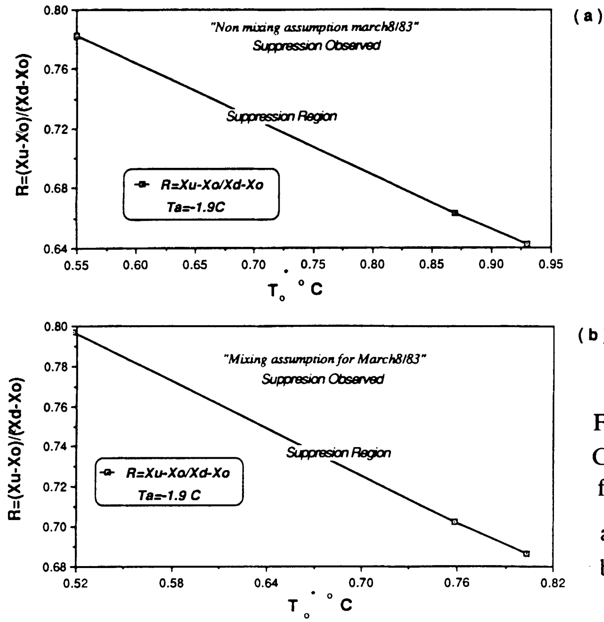

Fig. 7.
Calculated ice suppression ratio (R) for March 8;

a) non mixing;

b) mixing assumption.

calculations are presented below for March 8, 1983. On that day, an air temperature T_a of -1.9°C, and an daily average mixing temperature $T_0{}^* = 0.78$°C were recorded.

The first type of calculations was first used to evaluate the value of downstream distance to the ice edge (x_d-x_m), and the upstream distance to the ice edge (x_u-x_m) in the upstream direction. The ratio R corresponding to the daily average temperature $T_0{}^*$ is equal to 0.69 (< 1), indicating ice cover suppression, which was the case that day (Fig. 7a).

In the second type of calculation, the water temperature attenuation under the ice cover is calculated for Vaudreuil channel and St. Lawrence river up to the intersection of Beauharnois canal. The initial mixing temperature in front of Beauharnois, for March 8 is calculated using the following equation

$$T_0 \equiv \frac{Q.T(Vaudreueil) + Q.T(St.Lawrence)}{(Q\ Vaudreueil) + Q(St.Lawrence)}$$

which yields an daily average temperature of $T_0{}^* = 0.8$°C. The ratio R is then evaluated at 0.69, indicating ice cover suppression. Further calculations were also performed for several other days and the results were generally in agreement with the observed conditions. Those of the daily highest values of $T_0{}^*$ are summarized in Table 1, and other calculations are shown in Figs. 7 through 9.

By comparing both methods of calculation, it was found that the second method gives lower and more accurate values for (x_d-x_m) and (x_u-x_m), resulting in a better estimate of ice suppression, and more affirmative values for R. This is because the

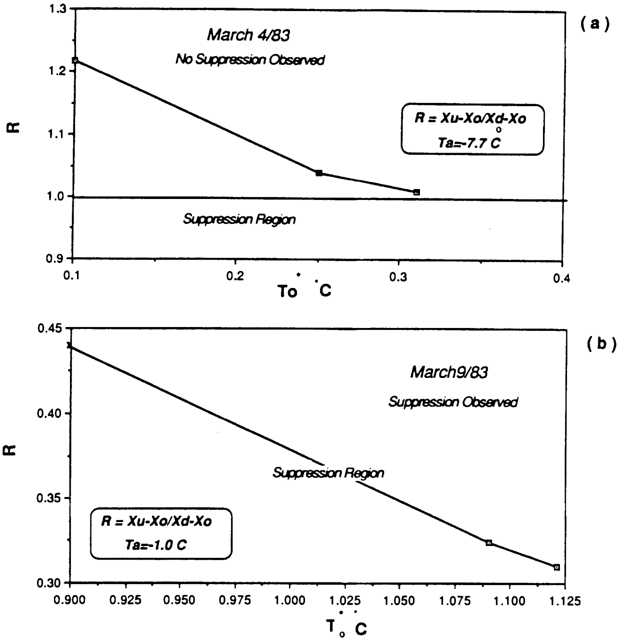

Fig. 8.
Conditions of ice cover suppression for March 4 and 9, 1983, with mixing assumption.

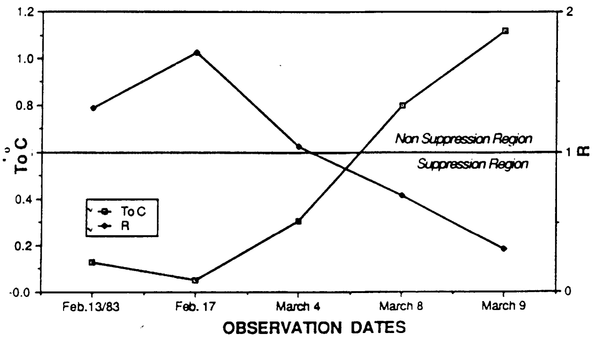

Fig. 9.
Interrelation between R and T_0* Calculated ice suppression ratio for various observation dates, (with mixing assumption).

Table 1 – Comparison between calculation and observation.

Date	T^*_0(^{0}C)	R (1) Calculated	T^*_0(^{0}C)	R(2) Calculated	Observations
Feb. 13/83	0.13	1.32	0.14	1.28	no suppression
Feb. 17/83	0.05	1.71	0.06	1.69	no suppression
March 4/83	0.31	1.04	0.35	1.01	no suppression
March 8/83	0.80	0.69	0.93	0.64	suppression
March 9/83	1.12	0.31	1.29	0.24	suppression

1–full mixing assumption ; 2–non-mixing assumption second method takes into consideration the effect of the colder water from the upstream tributaries of Vaudreuil channel and the St. Lawrence river. It is quite reasonable to assume that the particularly high velocity of water discharging from the power plant accentuates the mixing process between the effluent and receiving water. In addition, the geometrical configuration may also have played a role to increase the mixing process, and thereby, contributed in confirming the validity of the proposed formulation.

Conclusions

The upstream and downstream locations of the ice edge were investigated according to the 0°C isotherm criterion. Pertubation techniques based on the WKB approximation and Liouville-Green transformation were used in the formulations. It was assumed that the ice cover exists on the upstream section, and was subjected to suppression in the vicinity of a thermal effluent source.

The new criteria based on the ratio R provides a practical and reliable mean in predicting the ice cover suppression. Furthermore, the suppression of the ice cover was found to be a function of the flow velocity and the mixing rate of the thermal effluent discharge. Based on the calculations, it has been suggested that the thermal effluent with a higher temperature may not mix fully unless the velocity of the effluent stream is high enough to suppress the ice cover in the receiving stream. Comparison with the field data proves the validity of the above formulation as well as the proposed mixing formula, which take into account the water temperature from the colder water upstream of the point of discharge.

Acknowledgements

The authors with to acknowledge NSERC, and FCAR Funds (Canada) for the research grants under which this work was accomplished, and the hydraulics department of Hydro-Québec for supplying field data documentation.

Notation

C_p – specific heat ≡ 1.0 cal g^{-1} °C^{-1}
D – flow depth in meters
E_x, E_z – longitudinal and transversal mixing coefficients respectively, in m^2 sec^{-1}
h_{wa} – heat transfer coefficient at the water-air interface, in Wm^{-2}°C^{-1}
h_{wi} – heat tansfer coefficient at the water-ice interface, in Wm^{-2}°C^{-1}
Q_1 – water discharge in channel-1 in m^3/s
Q_2 – water discharge in channel-2 in m^3/s
R – hydraulic radius in meters
T_a – air temperature, in °C

T_1 – water temperature in channel-1 in °C
T_2 – water temperature in the side discharge channel, in °C
T_0 – initial water temperature upstream of channel-1 in °C
T_0^* – mixing water temperature at discharge point, in °C
T_e – water temperature at the ice edge, in °C
T_m – water temperature at water-ice interface assumed zero, in °C.
t – time, in seconds
u, v – mean flow velocity components in the x (longitudinal) and in z (transversal) directions respectively, in m s^{-1}
u_m – flow velocity at the mixing section, in m s^{-1}
x_0 – initial point upstream in channel-1 which is referred to as datum, in m
x_u – ice edge location, upstream of the point of discharge, in m
x_d – ice edge location downstream of the point of discharge, in m
μ – dynamic viscosity in kg m^{-1} s^{-1}
ϱ – density of water, in kg m^{-3}
Φ_{wa} – heat flux at the water-air interface
Φ_{wi} – heat flux at the water-ice interface

References

Anderson, E.R. (1954) Energy Budget Studies in Water Loss Investigation: Lake Henfer Studies, Technical Report, U.S. Geological Survey Professional Paper 269. pp. 71-118.

Ashton, G.D. (1984) River Ice Suppression by Side Channel Discharge of Warm Water IAHR, Montreal, Quebec.

Ashton, G.D. (1979) Suppression of River Ice by Thermal Effluents, Part I and II, USA Cold Regions Research and Engineering Laboratory, CRREL Report 79-30.

Calkins, D.J. (1984) Ice Cover Melting in Shallow River, Can. J. Civil Eng. II, pp. 225-265.

Dingman, S.L., Weeks, W.F., and Yen, Y.C. (1967) The Effects of Thermal Pollution on River Ice Conditions, I. Radiation, USA CRREL, Research Report 206, Dec.

Edinger, J.E., Duttweiler, D.W., and Geyer, J.C. (1968) The Response of Water Temperature to Meteorological Conditions, *Water Resources Research, Vol. 4.*

Hydro-Québec (1983) Campagne de mesures de glaces, Annexe (C), Prepared by Recherches B.C. Michel Inc.

Ince, S., and Ashe, G.W.T. (1964) Observations on the Water Temperature Structure of the St-Lawrence River, Proceedings of the Eastern Snow Conference, pp. 1-13.

Nyfeh, A.H. (1982) *Introduction to Perturbation Techniques,* John Wiley, New York.

Nyfeh, A.H. (1977) *Introduction to Perturbation Methods,* John Wiley, New York.

Paily, P.P., Macagno, E.O., Kennedy, J.F. (1974) Winter-Regimes Thermal Response of Heated Streams, ASCE J. Hyd. Div., No HY4.

Rohsen, and Choi, H.Y. (1961) *Heat, Mass and Momentum Transfer,* Prentice Hall Inc., Englewood Cliffs, N.J.

Address: Department of Civil Engineering,
Concordia University,
1455 de Maisonneuve Blvd. W.,
Montréal, Québec, Canada, H3G 1M8.

First received: 26 March, 1987
Revised version received: 14 August, 1987